Proceedings of the 7th International Symposium on Cavitation
CAV2009
August 17-22, 2009, Ann Arbor, Michigan, USA

CAV2009 – Paper No. 127

Numerical Simulation of Three-Dimensional Cavitation Bubble Oscillations by Boundary Element Method

Konstantin E. Afanasiev
Kemerovo State University
Kemerovo, Kemerovo region, Russia

Irene V. Grigorieva
Kemerovo State University
Kemerovo, Kemerovo region, Russia

ABSTRACT

This work is devoted to a numerical investigation of three-dimensional cavitation bubble. Bubble oscillations in ambient unbounded fluid are investigated numerically. The fluid is assumed inviscid, incompressible and unbounded and the flow is irrotational. The boundary integral method is used as an instrument of numerical investigation. Much attention is paid to the description of a numerical algorithm.

INTRODUCTION

This work is devoted to a numerical investigation of three-dimensional cavitation bubble oscillations. The fluid is assumed inviscid, incompressible and unbounded and the flow is irrotational. The problem is solved in full nonlinear three-dimensional statement. Produced results of numerical simulation compare with known analytical estimation.

The problem of bubble dynamics has long been an important research field. Both theoretical and experimental approaches have been applied to investigate this problem; and finally the preferred approach has become a numerical experiment. Due to the complexity of this problem, methods applied for its solution also vary considerably. Application of the finite-element method to problems of bubble evolution is described in [1, 2], of the volume-of-fluid method in [3], of the Langrange-Thomson method in [4], the generalized vortex method in [5], boundary integral method in [6].

The boundary integral method is used as an instrument of numerical investigation in this work. The particularity of this work is using of uncoordinated isoparametric linear approximation of velocity potential and its normal derivative on triangular mesh elements. This approximation was used in finite element method [7]. The advantages of the approximation in finite element method are well-known and described [7]. Authors do not know any other works dedicated to using of this approximation in boundary element method. Since the present work was started rather long ago [8, 9], the numerical algorithm has been thoroughly investigated. The conservative nature of the numerical algorithm can be tracked by controlling the conservation of energy.

THEORY

Let us consider transient fluid area $\Omega(t)$ bounded by bubble surface $\Gamma(t)$. The fluid is assumed inviscid and incompressible and flow is irrotational. In the case under consideration we study a model of a cavitation bubble and assume that the bubble is so small that the influence of gravity can be disregarded. The pressure inside the bubble is the sum of the saturated vapor pressure p_v and the pressure of the gas which, as we will assume, follows the adiabatic law $p_g = p_0 (V_0 / V(t))^{\lambda}$, where $V(t)$ is the bubble volume, p_0, V_0 are the initial gas pressure and bubble volume and λ is the ratio of specific heats. We neglect gas diffusion through the bubble boundary, i.e., the pressure on the bubble boundary $\Gamma(t)$ is defined as $p_\Gamma = p_v + p_g$.

In the initial moment of time the bubble is a sphere S_0 of the radius R_0. It is known from the experimental data that the bubble maintains its shape close to spherical for the most of its lifetime. There is a mathematical problem description for the velocity potential φ in nondimensional variables. The velocity potential satisfies Laplace's equation

$$\Delta\varphi = 0, \qquad x \in \Omega(t) \tag{1}$$

and the kinematical and dynamical conditions :

$$\frac{dx}{dt} = \nabla\varphi, \quad \vec{x} \in \Gamma(t), \tag{2}$$

$$\frac{d\varphi}{dt} - \frac{1}{2}|\nabla\varphi|^2 - 1 + \beta\left(\frac{V_0}{V}\right)^{\gamma} = 0, \quad \vec{x} \in \Gamma(t). \qquad (3)$$

The parameters are scales with respect to R_m for lengths, where R_m is the maximum radius that the vapour bubble would attain in an infinite fluid domain at a uniform pressure of p_∞, $R_m\sqrt{\rho/\Delta p}$ for time, where $\Delta p = p_\infty - p_v$ and ρ is a liquid density, $\sqrt{\Delta p/\rho}$ for velocity and $R_m\sqrt{\Delta p/\rho}$ for potential, and $\beta = p_0/\Delta p$.

The problem (1-3) is supplemented by the condition that fluid is quiescent at infinity (4).

$$|\nabla\varphi| \to 0, \quad |\vec{x}| \to \infty. \qquad (4)$$

Futher, it is necessary to specify the free-boundary location at the initial moment of time $t = 0$ and the potential distribution on it

$$\Gamma|_{t=0} = \Gamma_0, \quad \varphi|_{t=0} = \varphi(0, \vec{x}). \qquad (5)$$

Therefore, the boundary-value problem of the gas-vapor bubble evolution is described by equation (1) with boundary conditions (2-4) and initial conditions (5). The problem is nonlinear because of nonlinearity of the dynamical condition and the unknown location of the free boundary for $t > 0$. We seek to calculate the fluid motion and the location of the bubble surface $\Gamma(t)$ on $t > 0$.

NUMERICAL SIMULATION

The nonlinear boundary-value problem (1-5) may be reduced to a sequence of linear problems at each time step. To achieve that, one must execute a transition to a finite-difference approximation of time derivatives with the variable step Δt_j in the boundary conditions (2, 3), where j denotes the number of the time step. The time step is selected automatically and based on the condition that the mesh points can not be moved further than the prescribed distance:

$$\Delta t_j \le \frac{\varsigma l^j_{\min}}{\max_i |\Delta\varphi(\overline{x}_i, t)|},$$

where i is the mesh-node number, $l^j_{\min}$ the minimum lengths of the mesh edge and ς the empirical coefficient which should be selected so that the estimated time of bubble collapse coincides with the well-known analytical solution of the Rayleigh problem [10]. The time step depends directly on the kind of mesh approximating the bubble surface, and on the velocity of its motion. For example, for a mesh consisting of 602 nodes and 1200 elements, we have ς =0.0102. The method of mesh generation is described below. Naturally, there are values $\Delta t_{\min}$ and $\Delta t_{\max}$ which limit the maximum and minimum time step: in our case $\Delta t_{\min}$ =0.0001 and $\Delta t_{\max}$ =0.01.

To solve the problem (1) with the boundary conditions (4) and (5) we apply a boundary-element method, the third Green formula being invoked as its basic relation

$$C(x)\varphi(x) + \int_\Gamma \varphi(x,\xi)q^*(x,\xi)\,d\Gamma(\xi) =$$

$$= \int_\Gamma q(x,\xi)\varphi^*(x,\xi)\,d\Gamma(\xi),$$

where $q = \partial\varphi/\partial n$, φ^* is the fundamental solution of the Laplace equation, which is written in the spatial case as $\varphi^* = 1/(4\pi|x-\xi|)$; here x is the collocation point and ξ - current point on the boundary Γ; $q^* = \partial\varphi^*/\partial n$.

The bubble surface Γ is approximated by a set of plane triangular elements. Let us consider two different approaches to building a surface boundary-element mesh. In the first approach the initial surface is divided into separate triangular supporting zones. Each of the supporting zones imaged into the canonical domain is divided into a prescribed number of elements. Backward transformation allows forming the required surface mesh [11]. The number of mesh nodes N and elements M are determined by the number of zones and by partition of each separate zone. While the first approach is universal, the second is suited specifically for building a mesh on the surface of a sphere. The initial approximation of the sphere for the second algorithm is an icosahedron, each edge of which is bisected by a new mesh node. The obtained nodes are moved onto the surface of the sphere and combined into a new element. At each new discretization level, each element of the preceding level is transformed into four new elements. In this case, the number of mesh nodes and elements increases very rapidly, *viz.* $N = 5\times 2^{2n-1} + 2$, $M = 5\times 2^{2n}$, where n denotes the level of discretization; hence, we obtain only one acceptable computational mesh consisting of 642 nodes and 1280 elements. The advantage of the second approach is that the mesh, built by means of it, is more uniform; thus, in the first case, the ratio of the largest square of an element to its smallest square tends to 1.85, in the second case to 1.3. However, using the more regular mesh does not provide any noticeable advantage, even for calculations with sufficient deformation of the bubble boundary.

Let us suppose the functions φ and q are linear functions on the elements. A local system of coordinates is introduced on the elements (Figure 1); then $\overline{r} = x_3\overline{i} + y_3\overline{j} + z_3\overline{k} + +l_1\xi_1\overline{e}_1 + l_2\xi_2\overline{e}_2$, where l_1, l_2 are the lengths of the element sides, and $\overline{e}_1$, $\overline{e}_2$ denote unit base vectors of the introduced coordinates system with ξ_1, ξ_2 varying along the element side from 0 to 1 and $\xi_3 = 1 - \xi_1 - \xi_2$.

We use uncoordinated isoparametric linear approximation in this work. Classical linear approximation uses three nodes that disposed in the vertexes of triangular element (Figure 2a). Basis functions η_i $i = \overline{1,3}$ in this case are given by [12]

$\eta_i = \xi_i$.

In case of uncoordinated linear approximation nodes are in the middles of sides of triangular element (Figure 2b) and base function have another form [6] :

$$\eta_1 = \xi_1 + \xi_2 - \xi_3 = 2\xi_1 + 2\xi_2 - 1,$$

$$\eta_2 = \xi_2 + \xi_3 - \xi_1 = 1 - 2\xi_1,$$
$$\eta_3 = \xi_3 + \xi_1 - \xi_2 = 1 - 2\xi_2 .$$

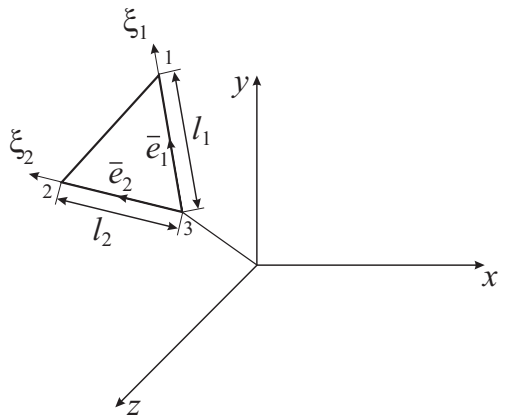

Figure 1. Local coordinate system on the triangular element.

Coordinates and approximated function will be written in the next form:

$$\overline{x}(\xi_1,\xi_2) = \sum_{i=1}^{3} \eta_i(\xi_1,\xi_2)\overline{x}_i ,$$
$$\varphi(\xi_1,\xi_2) = \sum_{i=1}^{3} \eta_i(\xi_1,\xi_2)\varphi_i ,$$
$$q(\xi_1,\xi_2) = \sum_{i=1}^{3} \eta_i(\xi_1,\xi_2)q_i .$$

Here $\overline{x}_i$, φ_i и q_i are the values of $\overline{x}$, φ and q in the i-th node.

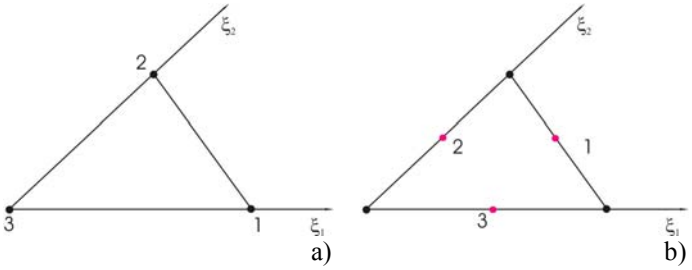

Figure 2. Flat triangular element;
a) classic linear approximation; b) uncoordinated linear approximation.

Boundary integral method uses uncoordinated linear approximation for counting normal derivatives in the nodes in the middles of element's sides. Then we have calculated normal derivatives in the nodes in the middles of element's sides we use these values for calculating velocity vector components in the vertexes of elements and new dislocation of the elements on the next time step.

The integral coefficients of the boundary-integral method are written as follows

$$h_{ij}^k = \int_{\Gamma_j} q^*(x_i,\xi)\eta_k d\Gamma(\xi) = -\frac{S_j}{2\pi}\int_0^1\int_0^{1-\xi_2} \eta_k \frac{(\overline{r}_i,\overline{n})}{|\overline{r}_i|^3} d\xi_1 d\xi_2,$$

$$g_{ij}^k = \int_{\Gamma_j} \varphi^*(x_i,\xi)\eta_k d\Gamma(\xi) = \frac{S_j}{2\pi}\int_0^1\int_0^{1-\xi_2} \frac{\eta_k}{|\overline{r}_i|} d\xi_1 d\xi_2 .$$

Here i is the number of collocation points with $i = \overline{1,M}$, j denotes the element number with $j = \overline{1,N}$, S_j s the j-th element square, $k = \overline{1,3}$ the local node number on the element, $\overline{r}_i = (x - x_i, y - y_i, z - z_i)$ and $\overline{n} = (\cos\alpha,\cos\beta,\cos\gamma)$ denotes the normal vector for the j-th element.

When $\overline{x}_i$ does not belong to the element Γ_j, the integrals h_{ij}^k and g_{ij}^k are regular; in this case the inner integrals are calculated analytically, whereupon the obtained integrals are calculated by Gaussian quadrature at seven points.
When the node $\overline{x}_i$ is one of the vertices of the element Γ_j, the integrals h_{ij}^k and g_{ij}^k have a singularity. The integrals h_{ij}^k, have a strong singularity $1/|\overline{x} - \overline{x}_i|^3$, but make zero contribution to the resulting system of equations, since the kernel numerator is a scalar product of the vector lying in the element plane $\overline{r}_i$ and its orthogonal vector $\overline{n}$. The integrals g_{ij}^k have a singularity of the $1/|\overline{x} - \overline{x}_i|$ kind; in this case the inner integrals are calculated analytically, whereupon inner integral can be calculated as a sum $g_{ij}^k = I_1 + I_2$, where I_1 - regular integral calculated by seven-point Gaussian quadrature and I_2 is a singular integral calculated according to the L'Hospital rule. For example, in case $k = 2$ I_2 is given by

$$I_2 = \frac{1}{8}\ln\left(\frac{2\sqrt{AB} + C}{2\sqrt{AB} - C}\right),$$

where

$$A = (x_1 - x_3)^2 + (y_1 - y_3)^2 + (z_1 - z_3)^2 ,$$
$$B = (x_2 - x_3)^2 + (y_2 - y_3)^2 + (z_2 - z_3)^2 ,$$
$$C = 2((x_1 - x_3)(x_2 - x_3) + (y_1 - y_3)(y_2 - y_3) + (z_1 - z_3)(z_2 - z_3)) .$$

We obtain the coefficients H_{ij} and G_{ij} by adding h_{ij}^k and g_{ij}^k to the corresponding values of the potential and normal derivative for all collocation points. The coefficients C_i, can be determined from the following considerations. If the constant potential $\varphi = const$ is defined on the boundary, the flow through the boundary equals zero and $C_i = -\int_\Gamma q^*(x,\xi)d\Gamma(\xi) + 1$ for domains with an infinite boundary.

The matrix of the resultant system of linear equations $AQ = B$ is completely filled, asymmetrical and non-sign-determined. During the calculation of test problems, exact methods of solution of the system of linear algebraic equations (the Gaussian method with basic element selection) have been

used. Iterative methods (the Gauss-Seidel method, the nonlinear regularity method [13], iteration schemes of incomplete approximation [14]) have also been used. The most acceptable of them turns out to be the Gaussian method with major element selection and with the following iterative refinement from the IMSL Microsoft Fortran Power Station library.

Having calculated the velocity values $(\partial\varphi/\partial x_i, \partial\varphi/\partial y_i, \partial\varphi/\partial z_i)$, $i = \overline{1,N}$ in the mesh nodes being the vertices of plane triangular elements, we can find the new location of the bubble surface and the potential distribution on it. Let us consider the algorithm for the velocity calculation the i-th node. We calculate the velocity components in the local coordinate system for each element, one of the vertices being the i-th node. As tangential directions $\overline{s}_j$ and $\overline{\tau}_j$ for the j-the element we use the element sides included up to the i-th node. The derivatives for these directions are calculated as the finite differences

$$\partial\varphi/\partial s_j = (\varphi_{m_j} - \varphi_i)/|\overline{s}_j|,\ \overline{s}_j = (\overline{x}_{m_j} - \overline{x}_i),$$

$$\partial\varphi/\partial\tau_j = (\varphi_{k_j} - \varphi_i)/|\overline{s}_j|,\ \overline{\tau}_j = (\overline{x}_{k_j} - \overline{x}_i),$$

where m_j and k_j are the numbers of two nodes of the j-th element, the third vertex of which is the i-th node. For the normal direction we use the normal vector $\overline{n}$ averaged over all surrounding elements. The normal velocity is known from the boundary-integral method, that is, $\partial\varphi/\partial n_i = q_i$. The calculated vector $(\partial\varphi/\partial n_i, \partial\varphi/\partial s_i, \partial\varphi/\partial\tau_i)$ is rearranged for the Cartesian-coordinates vector $(\partial\varphi/\partial x_i,\ \partial\varphi/\partial y_i,\ \partial\varphi/\partial z_i)$. We take as a result the average of the velocity vector for the elements surrounding the i-th node. Introduction of the weight coefficients as the inverse values of the distances between the surrounding element centers [14] does not result in a more accurate calculation of the velocity.

In the present work we do not use any smoothing algorithms, neither for the bubble surface, nor for the potential values on it, although in some cases numerical instability of the bubble surface and early failure of the calculation occur; smoothing would probably allow such calculations to proceed. Rejection of the use of smoothing algorithms is motivated, first of all, by the fact that using them would result in distortion of the energy characteristics [15] and lead to violation of energy conservation, which in this case is given by [10]

$$E = 3\int_\Gamma \varphi\frac{\partial\varphi}{\partial n}d\Gamma + V\left(1 - \frac{\beta}{1-\lambda}\left(\frac{V_0}{V(t)}\right)^\lambda\right),$$

where E is the full energy.

In order to demonstrate the performance of the boundary-element method during one time step, we have used the problem of the motion of an absolutely solid sphere in an unbounded fluid domain [16]. To demonstrate the numerical algorithm as a whole, and the method of selecting the time step in particular, we have used the Rayleigh problem concerning the collapse of a spherically symmetric bubble. We have also made a comparison with calculations of the axisymmetric problem [17].

RESULTS

Let us consider the process of oscillations of a gas bubble in an unbounded fluid domain. At the initial moment of time the bubble is a sphere of radius $1R_m$ that maintains its spherical shape and is compressed down to the minimum radius under the influence of the hydrostatic pressure. The initial gas pressure, although small, increases with decreasing bubble volume, thereby resisting the moving boundary; bubble collapse is followed by its expansion and vice versa; the bubble evolution becomes oscillatory. In this case the motion of the bubble boundary is described by the Rayleigh equation

$$\xi\ddot{\xi} + \frac{3}{2}\dot{\xi}^2 - \beta\xi^{3\lambda} + 1 = 0,$$

where $\xi = R/R_m$ is the non-dimensional radius of the bubble, $\dot{\xi}$, $\ddot{\xi}$ are the non-dimensional velocity and acceleration of the bubble boundary, respectively. Khoroshev [10] has derived an approximate dependence of minimum radius on the content parameter β (for $\beta>0.3$)

$$\xi_{\min} \approx \frac{3\beta}{1 + 3\beta - \beta^{3/2}},$$

where $\xi_{\min}$ is the minimum non-dimension radius of the bubble, using a numerical integration, taking $\lambda = 4/3$ for simplification.

Since this model does not take account of energy losses, the bubble oscillations can last indefinitely. We can traverse only the finite number of oscillations during the numerical simulation, whereupon the numerics fail because of the development of numerical instability on the boundary. The number of pulsation we have received using uncoordinated isoparametric linear approximation for all β is more than when we use traditional linear approximation. Figure 3 provides dependencies of the bubble radius on time as obtained from a numerical simulation of the bubble-oscillation process for β=0.4 and 0.5, and Figure 4 for β from 0.6 to 0.9.

As we can see on Figures 3 and 4 then β increases pulsation frequency and amplitude decrease. It is interesting that calculations fail as a rule at the end of bubble growth phase. Figure 5 provides bubble forms for β=04, 05 and 06 at two different moments: the moment of last minimal value and for the moment before calculation fails. The surface mesh used for this calculation consists of 642 nodes and 1280 elements. On this figures we can see that numerical instability of the bubble surface develops from the mesh node that surrounded by five elements. Other nodes are surrounded by six elements. We can conclude than mesh regularity tremendously influence for stability of numerical scheme realized in this work.

There is a good accordance of numerically calculated average radius of the bubble with it's analytical estimation for the some first oscillations. For other oscillations we can observe an increase of pulsation amplitude that we account for

development of boundary instability. Nevertheless full energy variation of have not exceeded 1.5%.

CONCLUSION

This work is devoted to a numerical investigation of three-dimensional cavitation bubble oscillations. Produced results of numerical simulation show a good agreement with known analytical estimation. Therefore we can say that the method described in this work allows to model oscillations for long periods of bubble existence.

The boundary integral method used as an instrument of numerical investigation use uncoordinated isoparametric linear approximation of velocity potential and its normal derivative on triangular mesh elements. The advantages of the approximation in finite element method are well-known and described [7]. This approximation has shown better result than classic linear approximation and made calculating more stable.

REFERENCES

[1] Rogers J. C. W., Szymczak W.G. 1997, Computations of violent surface motions: Comparisons with theory and experiment. *Phil. Trans. R. Soc. London* A 355 pp. 649-663.

[2] Sussman M., Smereka P. 1997, Axisymmetric free boundary problems. *J.Fluid Mech.* 341 () 269-294.

[3] Lawson N.J., Rudman M., Guerra Aand Lion J.-L. 1999, Experimental and numerical comparisons of the break up of a large bubble. *Experiments in Fluids*, Heidelberg: Springer-Verlag 26 524--534.

[4] Van Der Geld C.W.M. 2002, On the motion of a spherical bubble deforming near a plane wall. *J. Engng. Math.* 42 91-118.

[5] Pozrikidis C. 2002, Numerical Simulation of Three-Dimensional Bubble Oscillations by a Generalized Vortex Method. *Theoret. Comput. Fluid Dyn.* 16 151-169.

[6] Wang Q.X. 1998, The evolution of a gas bubble near an inclined wall. *Theoret. Comput. Fluid Dyn.* 12 29-51.

[7] Temam, R. 1995, *Navier Stokes equations and nonlinear functional analysis*, SIAM, Philadelphia, PA.

[8] Goudov A.M., Afanasieva M.M. 1990, Modeling of Spatial Problems of the Ideal Fluid by the Boundary Element Method. In: *High Speed Hydrodynamics: Inter-University Collection of Scientific Works*, The Chuvash State University, Cheboksari pp. 15—24 (in Russian).

[9] Afanasiev, K. E. Grigorieva, I. V. 2005, "Numerical investigation of three-dimensional bubble dynamics", *J. Eng. Math*., Vol. 55, 65-80 (16).

[10] Levkovskij Y. L. 1978, *Structure of cavitation streams*, Sudostroenie, Leningrad (in Russian).

[11] Ghasemi F. Automatic mesh generation scheme. *Computing and Structures* 15 (1982) 613-626.

[12] Terentiev A.G., Afanasiev K.E. 1987, *Numerical methods in hydrodynamics*, Cheboksary: ChuvGU.

[13] Trushnikov V.N. 1979, One Nonlinear Regulating Algorithm and Some of Its Applications. *J. Higher Math. Phys.* 19 pp. 822--829 (in Russian)

[14] Afanasiev K.E., Goudov A.M. and Zakharov Yu.N. 1992, The use of iteration schemes of incomplete approximation in some problems of hydrodynamics. *Modelling, Measurement & Control*, B, AMSE Press. 46(4) 27--40.

[15] Afanasiev K.E., Samoilova T.I. 1995, Technique of using the boundary element method in problems with free boundaries. *Computing Technologies*, Novosibirsk 11(7) 19--37 (in Russian).

[16] Lamb H. 1947, *Hydrodynamics*. Moscow, Leningrad: OGIZ, State Publ. House 928 pp.

[17] Afanasiev K.E., Grigorieva I.V. 2002, The investigation of bouyant gas bubble dinamics near an inclined wall. In: G.G. Cherny *et al.* (ed.), *HSH-2002 International Summer Scientific School High Speed Hydrodynamics. Proceedings*, Cheboksary, Russia, p. 111-119.

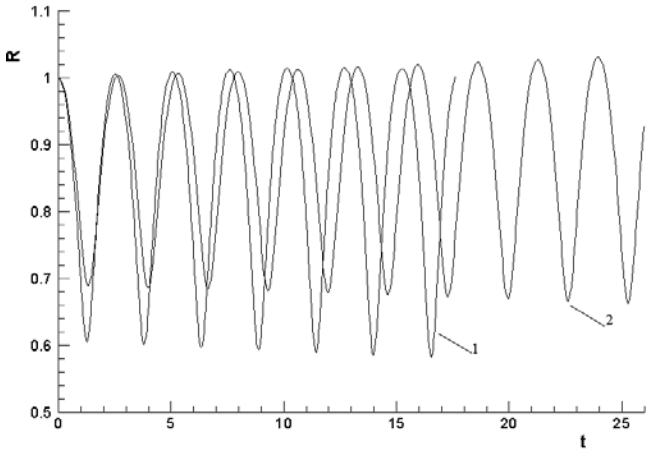

Figure 3. Graphs showing the dependence of the bubble radius on time for different values of β : 1 - β =0.4, 2 - β =0.5.

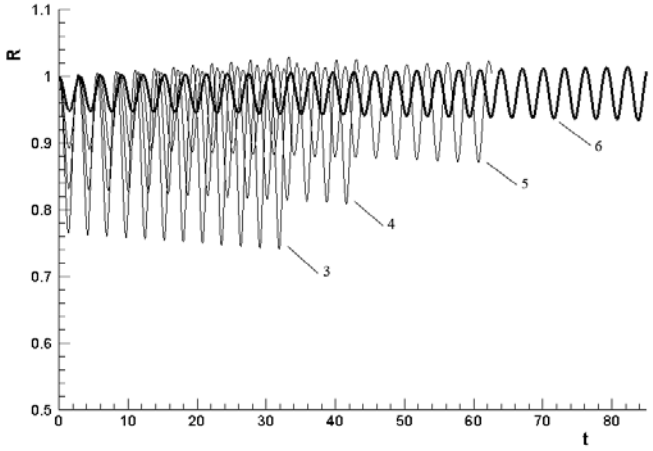

Figure 4. Graphs showing the dependence of the bubble radius on time for different values of β : 3 - β =0.6, 4 - β =0.7, 5 - β =0.8, 6 - β =0.9.

β =0.4

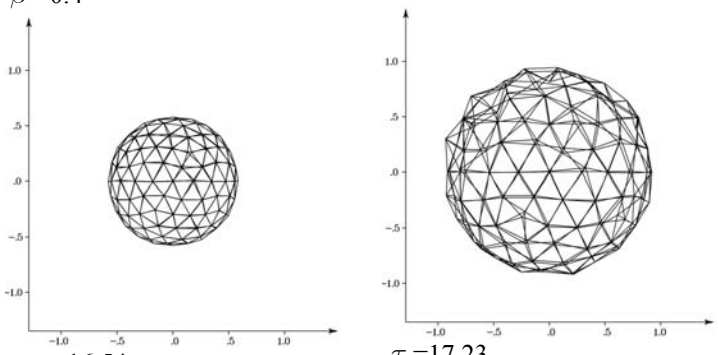

τ =16.54 τ =17.23

β =0.5

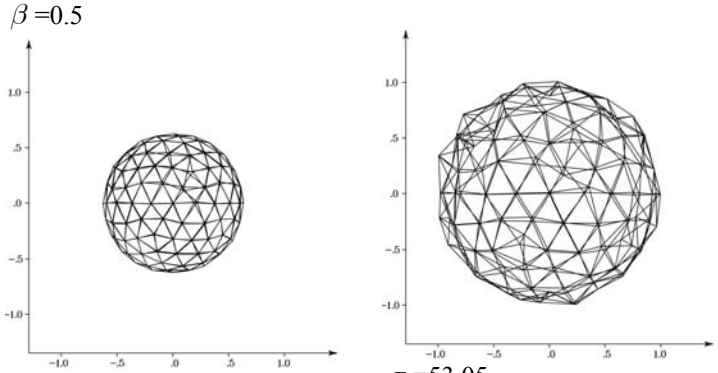

τ =52.08 τ =53.05

β =0.6

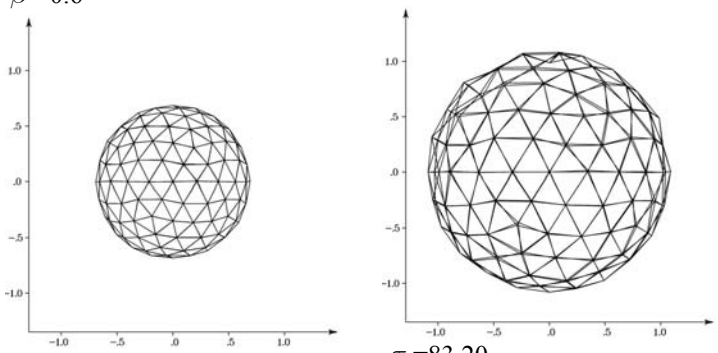

τ =81.94 τ =83.20

Figure 5. Shape of the bubble around minimal volume and at the last moment of lifetime for β =0.4, 0.5 and 0.6.